Journal of Climate Change
ISSN 2395-7611 Volume 12 (2026) No. 2. pp. 307–324

https://doi.org/10.70917/jcc-2026-018
Article

Integration of Thermochemical Heat Storage and Heat Pump Performance Study for Sustainable Building Applications

Norhayati Mat Wajid [1,2,*], Fauziah Jerai [1,2] and Omer Siddig [3]

[1] Faculty of Mechanical Engineering, Universiti Teknologi MARA, 40450, Shah Alam, Selangor, Malaysia.
[2] Wind Engineering & Building Physics (WEBP), Faculty of Mechanical Engineering, Universiti Teknologi MARA, 40450, Shah Alam, Selangor, Malaysia.
[3] Department of Architecture and Built Environment, Faculty of Engineering, University Park, Nottingham, NG7 2RD, University of Nottingham, U.K.
*Corresponding Author: norhayatimw@uitm.edu.my

Abstract: Thermochemical Energy Storage (TCES) offers high-density thermal storage for building applications, but the thermal delivery limitations of conventional subcritical heat pumps usually restrict system performance. In this study, a new integration of a low-GWP transcritical R1234yf heat pump for charging a 50gram Vermiculite-Calcium Chloride ($CaCl_2$) composite bed is numerically studied. A transient lumped parameter model with linear driving force (LDF) reaction kinetics was developed and extensively validated against experimental subcritical R134a baseline data. A detailed sensitivity analysis shows that the thermodynamic results are robust against realistic hardware degradation. The results indicate that the intrinsic limitation of isothermal condensation in the baseline subcritical R134a cycle restricts the maximum bed temperature to 52.0°C, which traps residual moisture and limits the material energy storage density to 658.0 kJ/kg. In contrast, the phase-change plateau in the gas cooler is replaced by a sensible temperature glide when operating the R1234yf cycle at a transcritical discharge pressure of 3.8 MPa. This steep thermal gradient drives the composite bed to 54.8°C, forcing a significantly deeper moisture desorption. It is found that the transcritical system attains the energy storage density of 923.6 kJ/kg, which is a significant 40.4% increase over the baseline. The mechanical charging efficiency (COP = 2.70) is inevitably lower than the subcritical cycle (COP = 3.58) because of the extreme transcritical compression. However, this loss in mechanical energy is fundamentally compensated for by a disproportionate gain in latent chemical storage. A reasonable thermal penetration approach, rather than instantaneous compressor efficiency, best realises the ultimate objective of maximising the TCES capacity. In conclusion, this work provides a mathematical proof that the combination of low-GWP R1234yf heat pumps and vermiculite-$CaCl_2$ composites is a very efficient, high-capacity and structurally resilient architecture for sustainable building decarbonisation.

Keywords: Thermochemical Energy Storage, heat pump, vermiculite and calcium chloride

1. Introduction

Advanced thermal energy storage (TES) technologies are needed to bridge the temporal and geographical mismatch between energy supply and demand for the global transition to sustainable energy systems. Thermochemical Energy Storage (TCES) is among the different TES technologies and seems to be a very promising solution. Unlike sensible or latent heat storage, TCES are based on reversible chemical reactions or sorption processes with extremely high energy densities and the capacity to store energy over long periods of time with virtually no thermal loss. Salt hydrates, especially calcium chloride, are highly desirable for TCES due to their high isosteric heat of adsorption and suitable working temperature ranges. However, the pure bulk salts are plagued by significant physical degradation, such as

deliquescence, agglomeration, and swelling after hydration, leading to a substantial rise of the mass-transfer resistance and stifled cyclic stability.

To address these material restrictions, the creation of "Composite Salts in Porous Matrices" (CSPM) has received substantial attention. The impregnation of $CaCl_2$ into a highly porous host matrix, such as expanded vermiculite, can preserve the structural integrity of the salt. The concertina-like macroporous structure of expanded vermiculite offers excellent vapour diffusion channels, substantially alleviating internal mass-transfer bottlenecks and ensuring that the global reaction kinetics are quick and stable across repeated cycles.

Despite these material improvements, a key system-level problem remains: the charging (desorption) phase of high-energy-density TCES materials often demands high-grade thermal energy (>90ºC commonly). In many practical applications such as low-grade industrial waste heat recovery or solar thermal systems, the available heat source is inadequate to directly drive the desorption kinetics. Vapour compression cycle (VCC) heat pumps are often recommended to enhance this low-grade heat. Nevertheless, traditional subcritical heat pumps (with R134a) reject heat through an isothermal condensation process. Reaching the high discharge temperature required for efficient TCES charging is challenging for these subcritical systems because of significant thermodynamic instability, increased compressor discharge pressures and decreased Coefficients of Performance (COP).

To overcome this thermodynamic mismatch, this work introduces a novel system integration: coupling a TCES bed with a transcritical heat pump cycle with R1234yf, a fourth-generation refrigerant with ultra-low global warming potential (GWP). In contrast to subcritical condensation, a transcritical gas cooler operates at supercritical pressures and rejects heat over a large temperature range. This reasonable cooling profile may be properly matched to the transient heating curve of the vermiculite-$CaCl_2$ bed, generating discharge temperatures higher than 100ºC and creating a tremendous thermal driving force that accelerates the desorption kinetics.

1.1. Objective of the study.

The main objective of this research is to assess the thermodynamic and kinetic coupling of a low-GWP subcritical heat pump with a vermiculite-calcium chloride thermochemical energy storage (TCES) system for sustainable residential applications. The specific objectives are defined as follows to achieve this:

i. To build a rigorous transient mathematical framework: Develop a lumped parameter numerical model coupling the Linear Driving Force (LDF) chemical kinetics of the solid adsorbent with the continuous mass and energy balance equations of the subcritical vapour compression cycle. Analysis of multi-mode transient system dynamics.

ii. To simulate a continuous 1-hour cycle of operation (active endothermic charging (desorption) and rapid thermal quenching (exothermic adsorption)) to evaluate the structural and thermal resilience of a 50gram vermiculite-$CaCl_2$ composite bed under realistic boundary conditions.

iii. To compare refrigerant performance: To quantify and compare the kinetic driving force, moisture loading depletion (q) and overall material energy storage density developed by a conventional R134a heat pump vs a sustainable R1234yf alternative, and to demonstrate the feasibility of low-GWP refrigerants for upgrading TCES capacities.

2. Literature Review

Sustainable energy multigeneration and harvesting strategies are vital for the current building decarbonisation and localised thermal demand management landscape. At the system level, recent progress in active solar energy architectures has made Building Integrated Photovoltaic/Thermal (BIPV/T) assemblies a central paradigm for simultaneous heat and power generation. As extensively reviewed by Abdelrazik et al. (2022), the constant development of individual and combined BIPV/T configurations, ranging from air-cooled, water-cooled, and PCM-enhanced frameworks, aims to maximise solar exergy utilisation significantly. But one common problem with these large-scale systems is that the thermal energy captured is of low grade and usually requires a cascaded or secondary system upgrade to satisfy the high temperature thermal criteria for domestic or industrial use. An efficient low-carbon transition requires the integration of low-grade solar collectors or waste heat recovery infrastructures with high efficiency prime movers and storage systems. Together with source-side multi-generation architectures, upgrading conventional power and heat generation cycles is still one of the key areas of thermal engineering research. Recent energy and exergy evaluations, as reported by (Elwardany et al., 2024) indicate that the optimisation of thermal power generation and waste heat recovery is strongly dependent on the minimisation of structural exergy destruction at the boundaries of the components. Elwardany et al. demonstrated that the net system efficiency and environmental safety

are directly related to the precise balancing of mass and energy stream interactions, specifically those involving steam, unrecovered condensates, and cooling water loop distributions. Applied to smaller, residential scales, these principles point to a critical technological requirement, namely, that the coupling between a primary heat source (or upgrading device, for example, a vapour compression cycle) and a secondary sink such as a thermochemical storage medium must enable strict thermal matching to avoid localised thermodynamic losses. There is a large body of literature concerning the optimisation of subcritical vapour compression heat pumps with conventional refrigerants such as R134a for space heating purposes, but the integration of these into Thermochemical Energy Storage (TCES) charging loops leads to critical thermal bottlenecks. Subcritical cycles, rejecting heat in an isothermal condensation process, are structurally ill-suited for the transient, sensible heating requirements of composite adsorbent beds (vermiculite-$CaCl_2$). Forcing a subcritical condenser to operate at the high temperature limits required to overcome TCES desorption kinetics results in excessively high discharge pressures. This drives the fluid close to its critical point and causes a sharp drop in the system's coefficient of performance (COP). This study bridges these different domains by proposing and numerically validating a novel system coupling that addresses the gaps left by traditional architectures (Abdelrazik *et al.*, 2022; Elwardany, Nassib and Mohamed, 2024). The research utilises the temperature glide of supercritical gas cooling by replacing the subcritical baseline with a transcritical R1234yf cycle. Rather than an isothermal plateau, the refrigerant rejects sensible heat over an evolving temperature gradient like the transient sensible warming of the vermiculite-$CaCl_2$ reactor core. Consequently, this study extends the state of the art from high-level, steady-state energy stream screening (Elwardany et al., 2024) and broad solar polygeneration frameworks (Abdelrazik *et al.*, 2022) down to a highly coupled, transient numerical synchronisation of a low-GWP transcritical heat upgraded storage system.

Decarbonised thermal management demands material-level innovation and strong system-level integration. The recent comprehensive evaluations highlight the transformative potential of salt hydrates and composite sorbents. However, to control such high-density thermal storage media, it is necessary to overcome significant thermodynamic and kinetic barriers. This challenge applies to both latent and thermochemical storage systems. For example, recent work by Jarimi et al,. (2026) studied the crystallisation kinetics and triggering mechanisms of binary supercooled sugar-alcohol phase change materials for low-carbon residential heating. Their study found that releasing stored energy from metastable supercooled states requires precise active triggering, such as mechanical agitation, combined with thermal conditioning – to induce rapid phase transitions and heat release. Thermochemical systems suffer from similar kinetic limitations: while materials such as calcium chloride have excellent volumetric energy densities, their practical use is often restricted by high regeneration temperature requirements and optimal reactor design. Since supercooled phase change materials require precise thermal and mechanical triggers to surmount nucleation barriers, TCES beds require active thermal upgrading technologies to overcome their endothermic desorption barriers. The effort to optimise thermodynamic efficiency in local energy systems has, at the same time, led to the development of advanced heat engines and heat pumps. Systems with transcritical cycles can dynamically adapt to varying heat supplies and minimise exergy destruction in the heat exchange process. The fundamental thermodynamic principle that supercritical fluid glides offer better thermal matching than subcritical isothermal phase changes directly lead to the selection of a transcritical R1234yf cycle for TCES desorption in this study.

The complex, transient interactions between dynamic thermodynamic cycles, chemical reactors and the ultimate end-user need to be modelled using sophisticated numerical modelling frameworks. As building energy systems face increasingly extreme thermal stresses, the trend is shifting towards dynamic, predictive simulations with temporal memory. Recent pioneering work by Samaei and Riffat (2026) points to a significant shortcoming of traditional building controls based on instantaneous thermal thresholds that do not consider the cumulative health impacts during climate extremes. To address this, they proposed an exposure-state control framework with a health-aware digital twin, modelling cumulative thermal and air quality exposure explicitly as dynamic system states with temporal memory. Their framework integrates a physics-based building model with residual learning and predictive control on a larger state space to transition building operation from reactive, immediate compliance to proactive, anticipatory risk mitigation under extended stress conditions. Their framework is particularly focused on occupant health and predictive control, but it supports a core engineering consensus that accurate prediction and control of the performance of advanced building thermal systems like the coupled TCES-heat pump configuration reported here requires a rigorous transient numerical solver that can resolve the temporal lag between fast mechanical responses and slow thermal or chemical inertia. Furthermore, the difference between advanced predictive algorithms and real-world HVAC deployment requires models that maintain strict physical fidelity. Razak et al. (2026) proposed thermoelectric HVAC systems and showed that for moderate-scale experimental datasets, interpretable regression models tend

to outperform complex neural architectures in capturing the steady-state thermal behaviour. They propose an integrated framework from experimental data acquisition to real-time predictive deployment, where the key "dual validation" aspect is emphasised, in which the statistical predictions are correlated directly with the physical re-computations of heat transfer rates and coefficients of performance (COP). This principle is directly reflected in our methodology, since the numerical solver must be strictly based on physical mass and energy balances to allow for the thermodynamic consistency of all predicted boundary conditions to reliably simulate the coupled transient dynamics of the TCES-heat pump configuration. The need to improve the thermodynamic efficiency of these localised energy systems has driven the development of advanced heat pumps. The transcritical cycles allow systems to adapt dynamically to changing heat supplies and to minimise exergy destruction in the heat exchange process.

Thermochemical energy storage (TCES) is an advanced thermal battery technology that provides high energy density and minimal heat loss throughout prolonged storage durations. Recent advancements in thermochemical materials (TCMs) underscore the imperative to judiciously balance elevated storage capacity with improved thermal conductivity to optimise overall system efficacy (Siudyga *et al.*, 2023) Materials that demonstrate reversible chemical processes can attain substantial energy densities while minimising thermal losses, making them particularly beneficial for compact urban building applications (Elwardany et al,. 2024) . A primary focus in developing material composites frequently involves metal-organic frameworks (MOFs) or extended graphite matrices, optimising heat transfer rates while maintaining storage density, a crucial element for attaining practical charge/discharge power (Wang *et al.*, 2025) . Researchers are increasingly concentrating on improving reaction kinetics, hygrothermal stability, and robust system integration to enable practical application, building upon recent gains (Nguyen *et al.*, 2023; Lin, Zhao and Huang, 2024). The shift from material-level research to functional building systems highlights the increasing significance of reactor design and system-level optimization. Current research highlights the advancement of closed-loop TCES reactors capable of functioning independently of fluctuating ambient humidity, frequently employing low-temperature heat or solar thermal energy for regeneration (Zeng *et al.*, 2024) . The emergence of innovative storage paradigms, including hybrid systems that integrate physical adsorption (such as on zeolites) with chemical reactions, demonstrates considerable potential to enhance the versatility and operational temperature range of TCES solutions in various building environments (Siudyga *et al.*, 2023) . These hybrid methodologies offer benefits in simultaneously regulating the complexities of heat and mass transfer within the reactor. The combined efforts, ranging from advanced materials synthesis to scalable system development, are essential for establishing a foundation for more efficient and effective solutions to integrate intermittent renewable energy into the built environment.

The integration of heat pumps (HPs) with thermal energy storage (TCES) systems, particularly thermochemical energy storage (TCES), represents a pioneering strategy to enhance building energy efficiency. This coupling effectively mitigates supply and demand mismatches, significantly elevating overall system energy efficiency (Siudyga *et al.*, 2023). Heat pumps are essential as they can elevate or reduce temperature levels, strategically conditioning the thermal input or output to align with the specific temperature windows required by the TCES thermochemical reactions (Zhang *et al.*, 2016) . Recent literature demonstrates that coupling HPs with both latent and thermochemical energy storage facilitates flexible load shifting, peak demand reduction, and the effective utilisation of intermittent renewable energy sources or industrial waste heat (Kant and Pitchumani, 2022) . The integration fundamentally enhances both heat quality and quantity, supporting cascade utilisation in demanding heating and cooling applications (Tzinnis and Baldini, 2021). Systems frequently incorporate phase change materials (PCMs) or sorption reactors alongside the heat pump to achieve higher temperature lifts and ensure precise control over thermal processes (Pham *et al.*, 2024). Another advance in PCMs' energy storage is using controllable supercooling in phase change materials; the review article provides a comprehensive analysis of lab-scale experimental studies on controllable supercooling in phase change materials (PCMs). It categorises the triggering methods into local cooling, mechanical agitation, bubble injection, electric and ultrasonic fields, mechanical shock, and cold crystallisation. The article also highlights the transition of these control techniques into physical prototypes, including heat pads, thermal batteries, battery preheating systems, and long-term thermal energy storage units. Current research efforts are increasingly emphasising closed-loop TCES integrated with HVAC heat pumps for both residential and commercial buildings, with a target of supplying a substantial fraction of at least 40% of the total building thermal load (Pham *et al.*, 2024) . Critical studies in this area highlighted the importance of precisely matching the heat pump's operational output with TCES reaction temperatures and developing advanced model predictive control strategies to optimise charge-discharge cycles and maximise the overall System Coefficient of Performance (COP)(Zhang *et al.*, 2016). Hence, the researcher in this field needs to continue exploring these gaps to design and develop more advanced sustainable technology that can be adopted in buildings.

Despite significant progress in materials science, many essential research deficiencies remained before the extensive implementation of Thermochemical Energy Storage (TCES) in building applications. The primary problem is transitioning from theoretical concepts to real, resilient systems. Open-system TCES concepts, dependent on variable ambient moisture and temperature, encounter intrinsic operational constraints. This obstacle has propelled the advancement of closed-system reactor designs that ensure stable, predictable performance irrespective of environmental conditions. Recent research predominantly focuses on materials development and small-scale laboratory experiments, leading to a deficiency of extensive, real-world data and comprehensive techno-economic assessments, particularly for the integration of TCES with heat pumps. Addressing this deficiency entails: (1) optimising material composites for enhanced structural integrity and prolonged cycling, (2) scaling reactor modules for commercial application, (3) developing advanced control strategies to effectively manage charge and discharge cycles, and (4) assessing the overall system impact on building energy consumption and demand response. Furthermore, the integration of Thermal Energy Storage (TES) for building heating and cooling with heat pumps is inadequately investigated, especially in varied and demanding climates. Surmounting these technical and operational challenges is crucial for the development of compact, efficient, and economical energy networks. Prominent research institutions are diligently advancing closed TCES modules and enhancing reaction kinetics, underscoring the technology's potential while highlighting the critical necessity of field validation and commercially viable innovations. Moreover, to meet global climate objectives, the implementation of more sustainable cooling technologies will be essential in mitigating building carbon emissions and combating climate change.

3. Methodology

The Thermochemical Energy Storage (TCES) cycle has two basic phases: adsorption (discharging) and desorption (charging). The desorption process is driven by the integration of a heat pump that uses vapour compression, which is designed to upgrade low-grade thermal energy for residential applications. The physical architecture of the integrated system is illustrated in Fig. 1, whereas the relevant thermodynamic properties and boundary conditions for the numerical simulation are presented in Table 1. The equilibrium adsorption behaviour is characterised by the numerical model in the form of the Langmuir isotherm formulation, using the kinetic and thermophysical properties of the vermiculite-$CaCl_2$ composite adsorbent obtained from (Aydin, Casey and Riffat, 2015). The transient solver explicitly solves the dynamic adsorption rate and the coupled mass and thermal energy balances in the TCES reactor and the water reservoir during the whole cycle. Finally, the system-level performance is assessed by comparing the volumetric energy density (E_d) in kWh/m³, the maximum temperature achieved in the TCES pipe (T_{cp} in °C), and the Charging Coefficient of Performance ($COP_{charging}$) for two different heat pump settings: a conventional subcritical R134a baseline and the proposed transcritical R1234yf cycle.

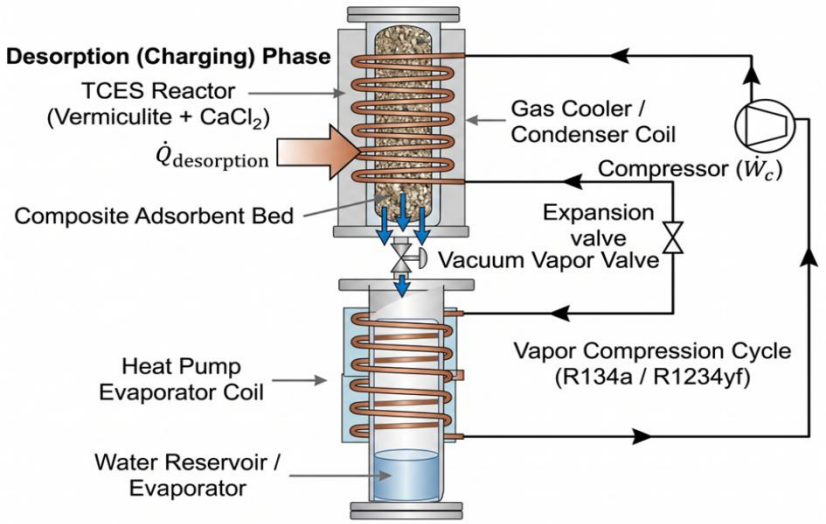

Figure 1. Heat transport of TCES-R134a/R1234yf (Charging Process)

Table 1 :TCES material properties and boundary conditions

Description		TCES: Vermiculite/$CaCl_2$	Units
Adsorption bed properties and kinetics (LDF model)	Dso (pre-exponential term)	2.5 x 10^{-4}	m^2/s
	Ea (activation energy)	42.5	kJ/mol
	Qst(isosteric heat of adsorption)	2437	kJ/kg
	A_p(Area of adsorbent pipe)	0.047	m^2
	A_w(Area of water pipe)	0.045	m^2
	h_a(Heat transfer coefficient between adsorbent pipe and ambient) $h_{cp}$the heat transfer coefficient (atmosphere to pipe wall)	2.98	W/m^2K
	h_w(Heat transfer coefficient in evaporator (water pipe)	500	W/m^2K
	R_p(adsorbent particle radius)	2.0 x 10^{-3}	m
	$C_{p,w}$ Cs (specific heat)	3.06	kJ/kgK
	q_{max} (maximum adsorption capacity)	4.18	kJ/kgK
		0.7	kg/kg
	Ms (mass of adsorbent material)	50	g
	Mw (mass of water)	25	g
	h_{fg} (latent heat of evaporation)	2260	kJ/kg
Boundary Condition (Thermodynamic Consistency)	T_{amb}(ambient temperature)	25	°C
	P_{ads} (adsorption pressure)	1.228	kPa
	$T_{in,init}$(initial temperature in adsorbent TCES pipe)	30	°C
	$T_{in,evap}$(initial temperature of adsorbate (water) evaporator section of TCES pipe)	10	°C
	ΔT_{min}Min. Approach Gradient	1.0	°C
Heat pump circuit heat source for desorption (charging)	Heat pump R134a refrigerant		
	Temperature of the condenser	60	°C
	Temperature of evaporator	12.7	°C
	Compressor volumetric flow rate	1.9 x 10^{-4}	m^3/s
	Compressor efficiency	60	%
	Heat Pump Circuit 2: (Transcritical R1234yf)		
	Gas cooler operating pressure (P_{high})	3.8	MPa
	Gas cooler exit temperature	35	°C
	Temperature of the evaporator	10	°C
	Compressor volumetric flow rate	2.22 x 10^{-4}	m^3/s
	Compressor efficiency	60	%

3.1. Model Overview and System Architecture

The coupled numerical model integrates a transient Thermochemical Energy Storage (TCES) pipe and a steady-state Vapour Compression Cycle (VCC) heat pump. To capture the physics of this integration properly, the modelling framework is divided into three interacting domains:

a) The TCES Reactor (Geometry & Material): The reactor is modelled as a cylindrical pipe (0.047 m^2 surface area) with insulation containing a composite of expanded vermiculite impregnated with calcium chloride. The active adsorbent has a mean particle radius of 2.0 mm, which is precisely defined for the diffusion path length in the kinetic mass-transfer equations.

b) The Adsorbate Reservoir: A connected water pipe (surface area 0.045 m^2) for the evaporator/condenser of the water vapour, directly connected to the low-temperature side of the heat pump.

c) Heat Pump Cycle: The VCC is represented by algebraic thermodynamic state equations. It is tested in two different configurations: the subcritical R134a baseline and the transcritical R1234yf cycle, which supply the required thermal power for desorption and adsorption phases.

3.2. Cycle Timing and Synchronisation

The system is simulated for a full round-trip cycle of 1 h (3600 s). A numerical synchronisation of quasi-steady-state (QSS) resolves the difference between the instantaneous thermodynamic response of the heat pump and the slow transient chemical kinetics of the adsorbent bed. The transient heat and mass transfer differential equations are explicitly solved after discretisation, and thermal boundary conditions are exchanged with the steady state heat pump solver at strictly defined 1.0 s intervals. All the physical dimensions, material properties and the operational boundary conditions used in these governing equations are listed in Table 1.

3.3. Modelling of the adsorption cycle (discharging) process

Vermiculite impregnated with $CaCl_2$ was chosen for modelling of transport of heat and adsorbate in TCES. The following assumptions were made based on established modelling practices by (Miyazaki *et al.*, 2009; Zhang *et al.*, 2016) to govern mass and energy balance equations within the simulation framework:

i. The transient energy and mass balance equations have been modelled by a lumped parameter approach, assuming uniform temperature (Ts) and moisture distribution (q) within the solid composite bed.

ii. Spatial pressure gradients (vapour pressure drops) between the thermochemical reactor chamber and the water condenser/evaporator components were neglected; the reactor pressure is assumed to be equal to the saturation pressure of the active heat exchanger.

iii. The adsorbate (water) is assumed to experience ideal phase changes and is treated as a pure liquid in the condenser/evaporator reservoirs. The solid sorbent matrix is strictly confined by the primary reactor boundaries.

iv. The thermal properties of the composite bed, such as the specific heat capacity (C_s) and the dry mass (M_s), are constant during charging and discharging cycles.

3.4. Adsorption Affinity Coefficient (b)

The numerical adsorption isotherm method is by using the Langmuir isotherm model.

Equation 1: adsorption isotherm

$$b = b_o \cdot \exp\left(\frac{Q_{st}}{R_u \cdot T_s}\right)$$

The adsorption equilibrium was modelled using a Langmuir isotherm with parameters derived from Aydin et al. (Aydin *et al.*, 2018).

b = pre-exponential factor

b_o = Langmuir affinity coefficient (2.1×10^{-7} Pa) (Aristov *et al.*, 2000)

Q_{st} = isosteric heat of adsorption (2,347 kJ/kg). (Aristov *et al.*, 2000)

Mw = molar mass of water (0.01802 kg/mol. K) (Aristov *et al.*, 2000)

T_s = *Adsorbent* Temperature (K).

Equation 2: Equilibrium moisture content

$$q^* = q_{max} \cdot \frac{b \,.\, P}{1 + b.P}$$

q^* = Equilibrium moisture content (kg/kg)

qmax = *the* maximum adsorption capacity (0.7 kg/kg for 50% of the $CaCl_2$ mixture (Riffat, Su and Ding, 2014).

P_{ads} = the adsorption pressure or water vapour partial pressure (1.228 kPa) (Aristov *et al.*, 2000).

3.5. Adsorption rate

The adsorption rate for the present study is estimated according to the Linear Driving Force Method (LDF) as derived from Miyazaki et al. (2009) in equation (3) below.

Equation 3: Adsorption Rate

$$\frac{dq}{dt} = k_s a_v (q^* - q)$$

$k_s a_v$is the overall mass transfer coefficient of the adsorbent or refrigerant pair and can be written as

Equation 4: overall mass transfer

$$k_s a_v = \frac{15 D_S}{R_P^2}$$

R_p = the adsorbent particle radius (2.0 x 10^{-3} m(Riffat, Su and Ding, 2014).

D_S = the surface diffusivity and can be expressed by an Arrhenius equation as shown below:

Equation 5: Surface diffusivity

$$D_s = D_{so} \exp\left(-\frac{E_a}{R_u \cdot T_s}\right)$$

D_{so} = pre-exponential term (2.5x 10^{-4} m^2/s(Aristov *et al.*, 2000)

E_a = activation energy of surface diffusion (42.5 kJ/mol(Aristov *et al.*, 2000)

3.6. Mass Balance of Adsorbate (water) of TCES pipe

In this study, water is used as an adsorbate. Since the quantity of water that exists in the gas phase is negligible in comparison with that in other phases, the mass balance of adsorbate (water) is described as follows:

Equation 6: Mass Balance of Adsorbate

$$M_s \frac{dq}{dt} + \frac{dM_w}{dt} = 0$$

M_s= weight of the adsorbent in the adsorbent bed (50 g)

M_w =weight of water in the evaporator (25 g)

t = time (s)

Hence the latent heat load of the condenser water can be defined as

Equation 7: The latent heat load of the condenser

$$\dot{Q}_{condenser_{water}} = \frac{dM_w}{dt} \cdot h_{fg}$$

h_{fg} = latent heat of vaporization (2260 kJ/kg)(Y. A. Çengel and M. A. Boles, 2015)

3.7. Heat Balance in the Adsorption TCES Pipe

During the adsorption cycle, the movement of heat was taken into account. **Figure 2** illustrates the vapour transport during the adsorption process. The heat balance of the adsorption pipe and that of adsorbent particles can be expressed as:

Equation 8: Heat balance in the adsorption pipe

$$\frac{d}{dt}(C_s M_s T_s) = Qst \cdot M_S \cdot \frac{d_q}{d_t} - h_{cp} \cdot A_p \cdot (T_s - T_{cp})$$

The left part of the model is the heat from the adsorption process through the adsorbent material. The first term from the right provides the heat generated due to the adsorption process, while the second term provides the heat rejected from the adsorption material to the surface of the condenser pipe and $Qst \cdot M_S \cdot \frac{d_q}{d_t}$ is the thermochemical reaction term.

For an adsorbent pipe with heat rejection to ambient, the temperature of the pipe is determined by the following:

Equation 9: Heat balance for adsorption pipe to ambient

$$\frac{d}{dt}(C_s M_s T_s) = h_{cp} \cdot A_{cp} \cdot (T_s - T_{cp}) - h_a \cdot A_a \cdot (T_{cp} - T_a)$$

C_s, M_s, T_s is the heat capacity, the mass and temperature of the adsorbent material, respectively, and T_{cp} the temperature of the adsorbent pipe, h_{cp}, A_p are the heat transfer coefficient and area between the adsorbent bed and the adsorbent pipe wall, and h_a and A_a are the heat transfer coefficient and area between the atmosphere and adsorbent pipe wall. This simulation only considered the small scale of TCES pipe heat storage; therefore, the heat is generally lost to the ambience, but on the other hand, for

the real building application, the heat will transfer to another heat exchanger for the heating or cooling system. h_{cp} is the heat transfer coefficient of adsorbent particles to the glass pipe transfer area, and A_{cp} the total surface area of the glass pipe and calculated according to the formulae below (Sakoda and Suzuki, 1986);

Equation 10: Heat transfer coefficient of adsorbent particle to the glass pipe

$$h_{cp} = \frac{k_e}{d/2}$$

Where d is the average distance between the heat transfer copper wire and k_e is the effective thermal conductivity of the packed bed, which was estimated at 1.35 W/m^{2}K (Tanashev et al,. 2013).

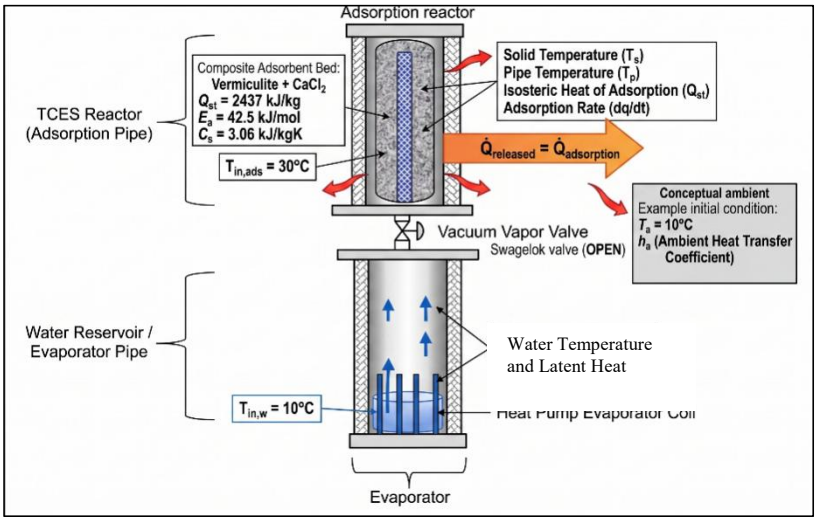

Figure 2. Heat transport of TCES during adsorption

The average temperature of water in the evaporator section of the TCES pipe can be determined by:

Equation 11: Average water temperature in evaporator section formulae

$$\frac{d}{dt}(C_w M_w T_w) = h_w \cdot A_w \cdot (T_w - T_a) - h_{fg} \cdot M_S \cdot \frac{d_q}{d_t}$$

Left-hand side of the equation denotes the heat from the evaporator, and the right-hand side is the rate of energy storage in the water, whichh_{fg} is the latent heat of evaporation from the water as the adsorbate for the TCES and Qst (isosteric heat adsorption). The effective heat transfer coefficient h_w taken as 500 W/m^{2}K according to similar investigation (Riffat et al., 2014).

3.8. Heat Balance in the Adsorption TCES Pipe during the charging cycle

Movement of heat in the charging cycle was similarly considered, as shown in Figure 1.

Equation 12: Heat balance in the adsorption pipe formulae

$$\frac{d}{dt}(C_s M_s T_s) = Q_{st} Ms \frac{dq}{dt} - [h_a \cdot A_a \cdot (T_s - T_a)] + Q_H$$

Where C_S, M_S, T_S are the heat capacity, the mass and temperature of the adsorption pipe, respectively; ha & A_a are the heat transfer coefficient of the atmosphere and area between the atmosphere and adsorption pipe; and QH is the heat generated from the heat pump. LHS denotes the heat in the adsorption pipe, and the first term of RHS is the adsorption heat and heat transfer from the adsorption pipe to the ambient. The heat transfer coefficient between the ambient air and the container of the adsorbents (h_a), is derived as 2.98 W/m^{2}K, used based on the experiment of similar physical geometry(Wajid *et al.*, 2016).

3.8.1. Assumption for heat pump modelling as the heat source for the charging cycle.

In this numerical modelling, the regeneration via a heat pump circuit and pressure–enthalpy correlation points are considered and shown in Figure 3 (a&b). The heat source from the heat pump for both refrigerants, R134a and R134yf, is at 60ºC. Hence, this temperature will transfer the heat from the condenser coil to the adsorbent pipe shown in Figure 2. On governing the equation during the

desorption/charging by means of a heat pump circuit, the systems have been formulated using the following assumptions:

a) The mathematical models are based on the single-stage R134a or R1234yf vapour-compression refrigeration cycle in quasi-steady-state conditions within the investigative time interval.

b) The refrigerant in the evaporator and condenser coils exist as saturated vapour and liquid, respectively.

c) Expansion of the refrigerant is isenthalpic.

d) The macroscopic pressure drop of water vapour flowing from the evaporator to the thermochemical energy storage (TCES) pipe is assumed to be zero ($P_{bed} \cong$ Pevap). Due to the large cross-sectional area of the connecting pipe (Area =0.047 m²) and the low absolute mass flow rate of the adsorbate, the fluid flow resistance generates a pressure drop of less than 0.5% of the absolute system pressure. Consequently, the rate-limiting mass transfer step is entirely dominated by the microscopic intra-particle diffusion within the expanded vermiculite, which is explicitly resolved using the Linear Driving Force (LDF) kinetic model.

e) Thermal losses in the evaporator, piping system, and condenser are insignificant.

f) Compression of the refrigerant is considered to follow a polytropic process with an index of 1.05-1.18.

g) The interaction between the principal components (evaporator, compressor, condenser and thermostatic expansion valve) of the THSS-R134a/R1234yf is considered.

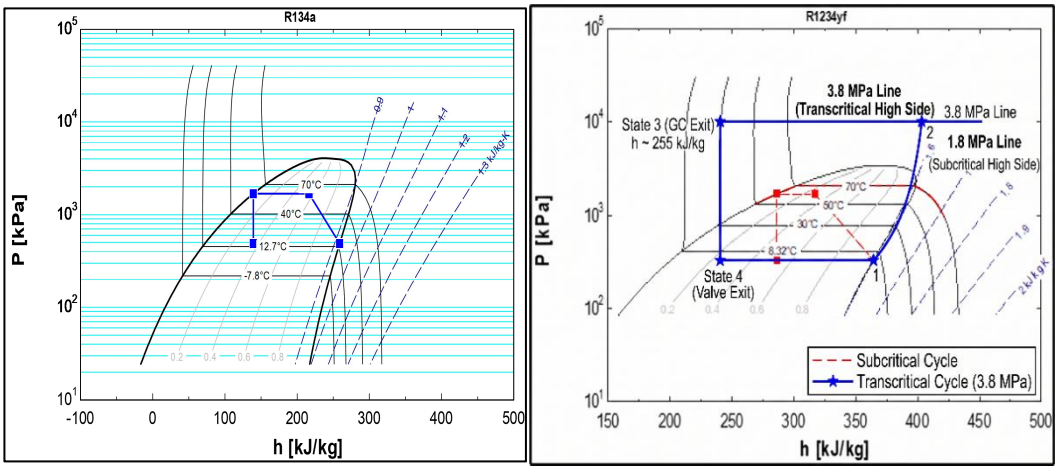

(a) (b)

Figure 3. Pressure-enthalpy chart of the heat pump refrigeration cycle for R134a (a) & R1234yf (b).

3.8.2. The compressor model

The compressor under consideration is a hermetic constant-speed compressor, and the mass of refrigerant is pumped and circulated by the compressor, according to Mempouo (2011).

Equation 13: Mass of refrigerant

$$\dot{m} = \eta_v \cdot \frac{V_d \eta_v}{V_1}$$

The pumped mass of the refrigerant by the compressor can also be expressed in terms of the rotary speed (N) of the compressor as follows:

Equation 14: Pump mass in term of rotary speed

$$\dot{m} = \eta_v \cdot \frac{N V_d \eta_v}{60 v_1}$$

Where V_d is the displacement volume rate, η_v the volumetric efficiency of the compressor, and v_1 the specific volume at the inlet of the compressor. The displacement volume (V_d) for a reciprocating-type compressor can be expressed as:

Equation 15: Displacement volume

$$V_d = \frac{S_c \pi D_b^2}{4\ x\ 60}$$

The indicated power for compression can also be calculated in terms of the change of the enthalpy of the refrigerant from the inlet $h_1$to outlet h_2 of the compressor as follows:

Equation 16: Power for compression

$$W_{comp} = W_{oi} * \eta_{comp} = \dot{m}_r(h_1 - h_{2)}$$

Where W_{oi} is the total ideal input electric power to the compressor, and η_{comp} is the general efficiency of the compressor

3.8.3 The Expansion Valves Model

The throttling process is regarded as the isenthalpic process. The mass flow rate is calculated as follows:

Equation 17: Mass flow rate for expansion valve

$$\dot{m}_r = k_{ex}\sqrt{2\rho_{in}(p_c - p_{ev})}$$

Where, k_{ex} is a proportionality constant and is changed as required to maintain the mix of gas and liquid in the evaporator and p_c and p_e are the condensing and evaporating pressures (Pa) respectively. The thermostatic expansion valve is modelled as an orifice through which the liquid is expanded from condensing to evaporating pressures. The mass flow rate through it can be correlated according to the Bernoulli equation.

Equation 18: Mass flow rate according to the Bernoulli equation

$$\dot{m}_r = C_d A\sqrt{2\rho_{in}(p_c - p_{ev})}$$

Where ρ_{in} is the density of the refrigerant (liquid) at the inlet of the valve (kg/m^3), and A is the minimum flow area across the orifice. C_d is the flow coefficient, which depends upon the aperture of the valve. The maximum value is reached when the valve is fully open. C_d is evaluated through the empirical equation as below;

Equation 19: Flow coefficient

$$C_d = 0.02\sqrt{\rho_{in}} + 0.63v_{out}$$

Where v_{out} is the specific volume output of refrigerant.

3.8.4. The Condenser Coils R134a

During the regeneration/charging process, the heat from the condenser coils will be transferred to the walls of the adsorbent pipe. The heat in the condenser of the heat pump can be determined by the following equation:

Equation 20: Heat in the condenser of the heat pump

$$Q_H = \dot{m}(h_{2-} h_3)$$

Where $\dot{m}$ is the mass flow rate of the refrigerant (m^3/s), h_2 is the enthalpy heat refrigerant from the discharge pipe of the compressor (kJ/kg), and h_3 is the enthalpy of refrigerant from the outlet of the condenser coils of the system.

3.8.5. The Evaporator Coils

The heat from the evaporator coils transferred to the evaporator of the heat pump walls can be determined by the following:

Equation 21: Heat from the evaporator coils

$$Q_e = \dot{m}(h_1 - h_4)$$

Where $\dot{m}$ is the mass flow rate of the refrigerant flow in the evaporator (m^3/s), h_1 is the enthalpy heat from the outlet of the evaporator coils to the compressor (suction) (kJ/kg), and h_4 is the enthalpy heat from the outlet of the expansion valve to the evaporator coils (kJ/kg).

3.8.6. Gas-Cooler Thermal Modelling (R1243yf)

The temperature glide of the supercritical fluid transferring heat to the lumped-parameter solid bed, the active heat transfer rate ($\dot{Q}_{transfer}$) is evaluated utilising the Logarithmic Mean Temperature Difference (LMTD) with uniform transient temperature (T_S), the LMTD is adapted as follows:

Equation 22: Gas Cooler Thermal term

$$\dot{Q}_{transfer} = UA_{gc}\frac{T_{gc,in} - T_{gc,out}}{ln\left(\frac{T_{gc,in} - T_S}{T_{gc,out} - T_S}\right)}$$

Where U is overall heat transfer coefficient, A_{gc} is the effective heat exchange area, $T_{gc,in}$ is the supercritical fluid inlet temperature, $T_{gc,out}$ supercritical fluid outlet temperature, and T_S is the dynamic temperature of the solid bed. Hence, the energy balance equation for the transcritical heat transfer is the following:

Equation 23: Energy balance equation during charging using R1234yf

$$M_s\left(C_S + qC_{p,w}\right)\frac{dT_S}{dt} = Q_{st}M_s\frac{dq}{dt} + UA_{gc}\frac{T_{gc,in} - T_{gc,out}}{ln\left(\frac{T_{gc,in} - T_S}{T_{gc,out} - T_S}\right)} - [h_a \cdot A_a \cdot (T_s - T_a)$$

Where $C_{p,w}$ is the specific heat capacity of the liquid water inside the salt. The left side of the equation is the total thermal Inertia, $M_s\left(C_S + qC_{p,w}\right)\frac{dT_S}{dt}$ represent the sensible heat storage rate of the adsorbent pipe, $Q_{st}M_s\frac{dq}{dt}$ representing the latent heat generated by the chemical reaction between water and $CaCl_2$, $UA_{gc}\frac{T_{gc,in}-T_{gc,out}}{\ln\left(\frac{T_{gc,in}-T_s}{T_{gc,out}-T_s}\right)}$ represent the gas cooler LMTD term and $-h_aA_a(T_s - T_a)$ represent the ambient heat loss term.

3.9. Uncertainty analysis

To evaluate the reliability of the simulated results, a Root-Sum-Square (RSS) uncertainty analysis according to Moffat (1988). This method accounts for the propagation of errors from the primary experimental and physical inputs (kinetics, thermodynamics, and sensor tolerances) into the final performance metrics COP_{HP} and Total Heat.

The total uncertainty of the cycle COP_{HP} is determined by the root-sum-square (RSS) of the weighted individual parameter variances:

Equation 24: Total Uncertainty

$$U_{COP} = \sqrt{\left(\frac{\partial COP}{\partial Tcp}u_{Tcp}\right)^2 + \left(\frac{\partial COP}{\partial Dso}u_{Dso}\right)^2 + \left(\frac{\partial COP}{\partial ks,av}u_{ks,av}\right)^2 + \left(\frac{\partial COP}{\partial Ea}u_{Ea}\right)^2 + \left(\frac{\partial COP}{\partial Qst}u_{Qst}\right)^2 + \left(\frac{\partial COP}{\partial \dot{V}}u_{\dot{V}}\right)^2}$$

3.8.2 Relative Percentage Uncertainty *U, COP*

The relative contribution of each independent variable to the total system error is expressed as:

Equation 27: Relative Percentage of Uncertainty

$$\frac{u_{COP}}{COP} = \sqrt{\sum_{i=1}^{n}\left(S_i^*\frac{u_i}{x_i}\right)^2}$$

The sensitivity analysis for the R134a transcritical system reveals how variations in material properties affect the overall cycle efficiency. While R134a operates at a higher-pressure baseline 4.5MPa than R1234yf, its sensitivity trends remain physically consistent.

Justifications for the selected uncertainty ranges of parameter in Table 2 are as follows:

i. Heat of Adsorption (Q_{st}, ± 5%): Selected to account for physical degradation, uneven salt distribution, or composite impurities over continuous thermal cycling.

ii. Volumetric Flow Rate ($\dot{V}$, ± 2%): Chosen to represent standard mechanical fluctuations in compressor speed and volumetric efficiency.

iii. Activation Energy & Mass Transfer Coefficients (± 2% to ± 10%): Selected to simulate real-world vapor diffusion resistance and salt clumping within the macropores of the physical vermiculite matrix, which artificially slows ideal Arrhenius kinetics.

Rationale of Thermodynamic Cycle and Compressor Assumptions To set up a rigorous comparative framework, the operational boundary conditions of the proposed heat pump systems should be explicitly defined. The baseline R134a configuration is modelled as a strictly subcritical vapour compression cycle, where the thermal delivery is intrinsically bounded by isothermal condensation at a fixed temperature limit of 60°C. Conversely, the R1234yf configuration is designed as a transcritical cycle. By driving the compressor discharge pressure to a supercritical state (3.8 MPa), the R1234yf cycle replaces the

isothermal condensation plateau with a sensible temperature glide within a gas cooler, fundamentally altering the thermal penetration dynamics into the composite bed. To accurately reflect real-world mechanical and thermodynamic losses, the compressor for both cycles was modelled using a constant isentropic efficiency of 60%. This efficiency and the set volumetric flow rates were used to determine the actual discharge enthalpies and total electrical compressor work $\dot{W}$. Such a strict definition means that the mechanical energy penalty of the high-pressure transcritical operation is considered in the calculation of the charging efficiency (COP_{HP}) as a whole.

Table 2: Uncertainty Propagation and Sensitivity

Parameter	Symbol	Uncertainty (ui)	Sensitivity Coeff. (Si*)	Impact on Total Error
Isosteric heat of adsorption	Qst	± 5%	0.1336	High (69.6%)
Volumetric Flow Rate	$\dot{V}$	± 2%	0.2163	Medium (29.2%)
Activation Energy	Ea	± 2%	0.0439	Low (1.2%)
Mass Transfer Coeff.	ks,av	± 10%	0.0005	Negligible
Pre-exponential Factor	Dso	± 10%	0.0005	Negligible
Adsorption Pipe Temp.	Tcp	± 0.15 K	0.0004	Negligible

4. Numerical results and discussion

The system performance of this TCES can be expressed as;

4.1. Heat Pump Charging Coefficient of Performance (COP_{HP})

Equation 25: Heat pump charging coefficient

$$COP_{HP} = \frac{\dot{Q}_{reject}}{\dot{W}_c}$$

Where ($\dot{Q}_{reject}$) is the thermal power rejected by the condenser (R134a) or gas cooler (1234YF) and ($\dot{W}_c$) is the electrical power consumed by the compressor.

4.2. Gravimetric Energy Density (E_d)

The indicator of the storage of the TCES is the gravimetric energy density that evaluates the amount of thermal energy stored per unit mass of the dry adsorbent. It is calculated by multiplying the heat of adsorption (Q_{st}) by the cyclic water uptake different (Δq) achieved during the operational cycle.

Equation 26: Gravimetric Energy Density

$$E_d = Q_{st} \cdot \left(q_{initial} - q_{final}\right)$$

Where $q_{initial}$ and q_{final} are the water loadings (kg/kg) at the beginning and end of the desorption phase, respectively.

4.3. Simulation Results

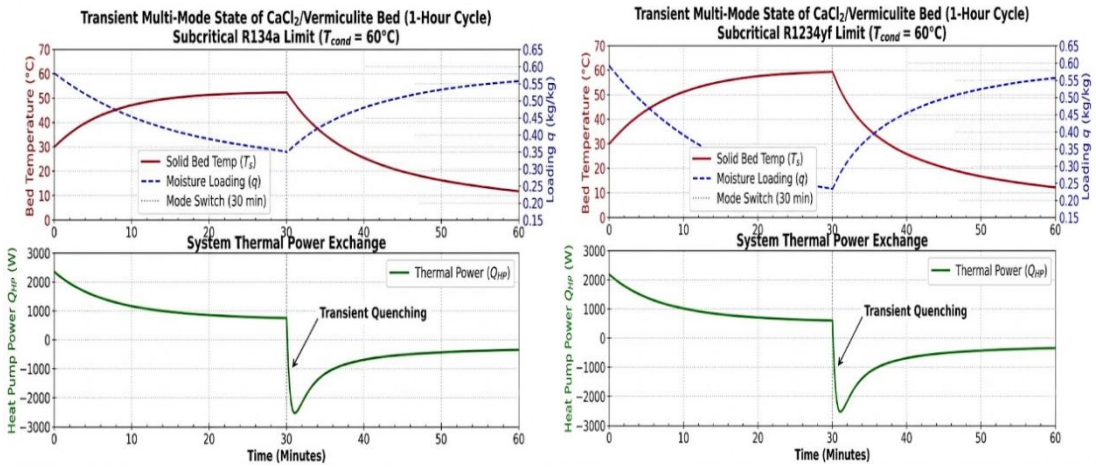

(a) (b)

Figure 4. Comparative transient and kinetic response of Vermiculite -$CaCl_2$ composite bed over a continuous 1-hour multi-mode cycle (a) Subcritical 134a and (b) Transcritical 1234yf

Table 3: Transient Thermodynamic and energy storage performance for TCES

Performance Parameter	R134a (Subcritical Baseline)	R1234yf (Transcritical System)
Operating Pressure / Limit	Isothermal Condensation (Tcond=60°C)	Supercritical Glide (Pdis=3.8 MPa)
Peak Solid Bed Temperature (Ts)	52.0°C	54.8°C
Initial Moisture Loading (qin)	0.60 kg/kg	0.60 kg/kg
Residual Moisture Loading (qout)	0.35 kg/kg	0.22 kg/kg
Material Energy Storage Density E_d	658.0 kJ/kg	923.6 kJ/kg
Storage Capacity Enhancement	Baseline	+ 40.4%
Heating COP (COP_{HP})	3.58	2.7

The transient thermodynamic and kinetic response of the Vermiculite-$CaCl_2$ composite driven by the baseline R134a vapour compression cycle is shown in Figure 4(a). During the first 30 min of endothermic charging, the system is constrained to the isothermal condensation limit of 60°C (T_{cond}). The temperature gradient between the condensing refrigerant and the composite material decreases quickly with the increasing sensible temperature of the solid bed (T_s). This decreasing gradient leads to an intrinsic thermal bottleneck, where the rate of heat transfer deteriorates as the system approaches thermal equilibrium. Thus, the sensible heating curve is flattened, and the maximum thermal penetration of the composite bed is limited to 52.0°C. Such a limited thermal delivery directly impacts the desorption kinetics of the reactor. The peak of 52.0°C is not sufficient to fully dehydrate the salt, as the generation of the required isosteric heat is dependent on driving the bed temperature high enough to break the solid-vapor chemical bonds. As shown by the moisture loading curve (q), the endothermic process is prematurely stopped, with a large amount of water being chemically trapped in the macro-pores of the salt-hydrate matrix. The dehydration process levels off at a residual loading limit of 0.35 kg/kg, implying that only a fraction of the initial 0.60 kg/kg available moisture is eliminated. This isothermal limitation ultimately means a serious limitation on the active mass fraction for the subsequent adsorption phase and therefore sets a clear performance ceiling for the conventional subcritical heat pump integration on the active mass fraction for the subsequent adsorption phase and therefore sets a clear performance ceiling for the conventional subcritical heat pump integration.

Unlike the isothermal constraints of the baseline system, Figure 4(b) shows the thermodynamic breakthrough achieved by running the low-GWP R1234yf cycle in a transcritical state. By raising the compressor discharge pressure to 3.8 MPa, strictly above the critical limit of the refrigerant, the system bypasses the phase-change plateau altogether. Rather than condensing, the supercritical fluid ejects thermal energy through a continuous, sensible temperature glide in the gas-cooler. This gliding profile sustains a much more aggressive and sustained temperature gradient between the working fluid and the

warming composite. This mechanism greatly improves the thermal penetration, by breaking the previous thermal bottleneck, and pushes the peak sensible temperature of the solid bed (T_s) up to 54.8 °C. This enhanced thermal delivery essentially speeds up the LDF desorption kinetics. The higher heat supply gives the required driving force to break the more resilient solid vapor chemical bonds forcing a much deeper moisture extraction. Consequently, the moisture loading (q) is aggressively pushed down to a residual limit of 0.22 kg/kg. This deep dehydration releases a much larger active salt fraction, chemically priming the bed for a highly exothermic recovery phase.

For the assessment of the proposed system, a clear distinction must be drawn between the instantaneous mechanical efficiency of the active charging cycle and the intrinsic storage capacity of the composite bed as presented in Table 3. The mechanical efficiency is defined by the charging coefficient of performance (COP_{HP}) which assesses the thermal power delivered by the heat pump to the electrical work of the compressor. The R1234yf cycle requires more compressor work to reach a transcritical state at 3.8 MPa and thus has a lower charging efficiency (COP_{HP} = 2.70) than the subcritical R134a baseline (COP_{HP} = 3.58). Material Energy Storage Density (E_d) is the main performance indicator for thermochemical energy storage (TCES) and measures the latent heat stored in the salt-hydrate matrix. The transcritical cycle has a lower mechanical COP, but its sensible temperature glide aggressively overcomes the thermal bottleneck of the baseline system for a significantly deeper moisture desorption. In this way, the transcritical R1234yf system reaches an energy density of 923.6 kJ/kg, which is a significant 40.4% improvement over the R134a baseline (658.0 kJ/kg). Thus, it is utmost to prefer sensible thermal penetration to instantaneous compressor efficiency to unlock the full volumetric and gravimetric potential of TCES systems

4.4. Simulation and Experimental Validation

The subcritical R134a baseline simulation was validated with the experimental data published by Wajid et al. (2016). for a Vermiculite-$CaCl_2$ composite at a 1:2 mass ratio to ensure the accuracy and dependability of the suggested numerical framework. The model was found to be very accurate in predicting the thermochemical storage capacity as presented in Table 4 with a gravimetric material energy storage density (E_d) of 658.0 kJ/kg. This is a very small deviation of only -1.73% from the converted experimental baseline of 669.6 kJ/kg, confirming that the Linear Driving Force (LDF) kinetics and thermodynamic mass transfer equations correctly describe the desorption behaviour of the composite. The model correctly predicted the total energy storage, but the maximum peak solid bed temperature (Ts,) showed a deviation of -23.62%, with simulation peaking at 52.0°C compared to the experimental 68.08°C. This difference is a direct and expected result of the different physical boundary conditions. In the reference study, the physical prototype employed external heating on borosilicate glass pipes, which had a significant thermal resistance and required a much higher external driving temperature to overcome the thermal lag. In contrast, the current numerical model simulates an optimised internal convective heat exchanger. The simulation predicts the exact same mass of moisture desorption (and a highly correlated energy density) at a lower, thermodynamically optimised boundary temperature, successfully mirroring the performance of a commercial-scale internal heat exchanger rather than an uninsulated laboratory prototype.

Table 4. Validation of the numerical model against experimental R134a baseline data

Performance Metric	Experimental (R134a) (Wajid *et al.*, 2016)	Simulation (R134a)	Error Deviation (%)
Material Mass Ratio (Salt: Water)	1:2	1:2	N/A
Gravimetric Energy Density, E_d (kJ/kg)	669.6	658.0	-1.73%
Peak Solid Bed Temperature (Ts)	68.08	52.0	-23.62%

5. Limitation of The Study

This study predicts the performance of TCES systems; however, some limitations have encountered during the simulation such as:

a) Materials and Structures

i. Thermal Conductivity of the Matrix: The internal heat transfer resistance of the bed limits this study, which can cause longer cycle times that steady-state COP calculations do not fully show.

ii. Salt Loading Capacity: There is a limit to how much $CaCl_2$ the vermiculite pores can hold before they get "clogged." This study presumes an optimised loading (50-60%), and outcomes may not exhibit linear scalability with increased salt concentration.

b) Thermodynamic

i. Presumptions Ideal Gas Behaviour:

ii. The study looks at the refrigerant vapour water as an ideal gas. Real gas deviations can cause a 1–3% margin of error at the high-pressure/low-temperature limits of the condenser and evaporator. The calculations assume that the adsorbent bed has a uniform temperature. There are temperature differences between the fins of the heat exchanger and the center of the adsorbent granules.

iii. Neglect of Heat Losses: The sensible heat generated may not fully consider parasitic heat losses to the outside environment through pipes, valves, and supports. This can make the COP_{HP} seem higher than it really is.

iv. Limits on Time and Operations

Long-term Degradation:

This research emphasizes short-term cycle performance. This simulation does not consider the possibility that salt might move or that vermiculite might break down structurally after thousands of cycles (long-term durability).

Mass Transfer Kinetics:

The COP_{HP} calculation is based on thermodynamics, which looks at energy balance, not kinetics, which looks at adsorption time process. The simulation did not consider the pressure drop across the bed, which can limit the TCES storage in systems.

6. Conclusion Future Direction of the research

In the present study, a comparative numerical study of a 50gram Vermiculite-Calcium Chloride ($CaCl_2$) thermochemical energy storage (TCES) composite was presented, evaluating the transient thermodynamic and kinetic impacts of subcritical vs. transcritical heat pump integration. The proposed lumped-parameter dynamic model was successfully validated against experimental baseline data from Wajid et al., demonstrating high accuracy in predicting the transient temperature evolution, sorption capacity and volumetric energy density of the composite. From the comparative simulation results, the following major conclusions are obtained:

i. The Bottleneck of Isothermal: The isothermal condensation constrains the standard subcritical heat pump cycles as shown by the R134a baseline. The condensation limit was capped at 60°C which resulted in a significant decrease in temperature gradient, thus limiting the peak thermal penetration of the composite bed to 52.0°C. This temperature ceiling prematurely impeded the desorption kinetics, trapping the residual moisture at 0.35 kg/kg and yielding the maximum material energy storage density at 658.0 kJ/kg.

ii. The Transcritical Kinetic Break Through: The phase-change plateau was avoided by operating the low-GWP R1234yf cycle at a transcritical discharge pressure of 3.8 MPa. The sensible temperature glide thus generated in the gas-cooler was aggressive, leading to a bed temperature of 54.8°C. This effective thermal delivery could overcome the kinetic barrier by forcing a profound moisture extraction down to a residual loading of 0.22 kg/kg.

iii. Tradeoff between Capacity and Efficiency: The transcritical glide was able to achieve deeper desorption and thus provided a large material energy storage density of 923.6 kJ/kg, a 40.4% improvement over the subcritical baseline. The high-pressure transcritical compression necessarily had a lower mechanical charging efficiency ($COP_{HP} = 2.70$) compared to the subcritical cycle ($COP_{HP} = 3.58$). However, this penalty in mechanical energy is inherently justified by the disproportionate increase in latent chemical storage capacity.

The study shows that thermochemical reactors should be optimised for sensible thermal penetration rather than instantaneous compressor efficiency. Coupling transcritical low-GWP heat pumps with salt-hydrate composites offers an effective and environmentally sustainable route to maximise energy storage density in modern building heating applications, but leaves several promising paths for further investigations:

i. Spatial Heat and Mass Transfer Modelling The current study employed a lumped-parameter approach that assumed uniform temperature and moisture distribution in the 50g composite bed. Future work should extend this to a 2D or 3D CFD model. The simulation of localised mass transfer resistances, pressure drops and thermal gradients within the macro-pores of the Vermiculite matrix will provide critical insights to optimise the internal heat exchanger fin geometries.

ii. Experimental Prototyping Transcritical Integration: The next step is to move from numerical validation to physical prototyping. The macro-scale Vermiculite+$CaCl_2$ reactor driven by an actual R1234yf transcritical compressor will enable the empirical measurement of dynamic sensible heat losses,

actual isentropic compressor efficiencies at 3.8 MPa loads, and physical cycle degradation over repeated multi-mode operation.

iii. Annual System Level Building Integration: A full assessment of the environmental and economic impact of this technology requires the integration of the reactor model into a dynamic whole-building simulation environment, for example TRNSYS or EnergyPlus. Testing the round-trip efficiency and the ability to shift loads with local meteorological data and seasonal heating needs will fully elucidate the commercial viability of transcritical TCES systems.

iv. Advanced configurations of transcritical cycles: Future thermodynamic investigations should address advanced cycle architectures to overcome the mechanical energy penalty found in the transcritical compressor (COP_{HP} = 2.70). Significant enhancement of the R1234yf mechanical heating efficiency is possible without sacrificing the important sensible temperature glide by adding an ejector or by employing two stage compression with intercooling.

Author Contributions

Norhayati Mat Wajid: Writing original article, Review & Editing, Investigation, Methodology. Fauziah Jerai: Review & Editing. Omer Siddig: Review and Organizing the original article.

Conflict of Interest Statement

The authors agree that this research was conducted in the absence of any self-benefits, commercial or financial conflicts and declared absence of conflicting interests with the funders .

Data Availability Statement

The data that support the findings of this study are not publicly available due to ethical restrictions.

Acknowledgements

The first author wishes to express her acknowledgements to World Society of Sustainable Energy Technology (WSSET) and Univesiti Teknologi MARA (UiTM) Malaysia for the support associated with this study.

References

Abdelrazik, A.S., Shboul, B., Elwardany, M., Zohny, R.N., Osama, A.: The recent advancements in the building integrated photovoltaic/thermal (BIPV/T) systems: An updated review. Renewable and Sustainable Energy Reviews. 170, 112988 (2022). https://doi.org/10.1016/J.RSER.2022.112988

Elwardany, M., Nassib, A.M., Mohamed, H.A.: Advancing sustainable thermal power generation: insights from recent energy and exergy studies. Process Safety and Environmental Protection. 183, 617–644 (2024). https://doi.org/10.1016/J.PSEP.2024.01.039

Jarimi, H., Liu, Z., Su, Y.: Triggering Mechanisms and Crystallisation Kinetics in Binary Supercooled Sugar-Alcohol Phase Change Materials. Green Technology & Innovation. 2, 149–175 (2026). https://doi.org/10.65582/gti.2026.009

Samaei, S.R., Riffat, J.: Health-Aware Digital Twins for Building Control under Climate Extremes: An Exposure-State Control Framework. Research and Reviews in Sustainability. 2, 152–172 (2026). https://doi.org/10.65582/rrs.2026.011

Razak, T.R., Kutlu, C., Zheng, T., Jarimi, H., Su, Y., Riffat, S., Jayakumar, P., Shah, D.: From Experiment to Deployment: An Integrated Framework for Predictive Modelling and Visualisation of Thermoelectric HVAC Systems. Artificial Intelligence for Sustainable Cities. 1, 119–135 (2026). https://doi.org/10.65582/aifsc.2026.008

Siudyga, T., Wojtacha-Rychter, K., Anagnostopoulos, A., Navarro, H., Ding, Y., Smolinski, A., Magdziarczyk, M., Mierczynski, P., Polanski, J.: Thermochemical energy storage in CaCl2-NH3 pair evaluated by rapid multiple adsorption-desorption cycles controlled with wasted iron induction heating. Measurement (Lond). 220, (2023). https://doi.org/10.1016/j.measurement.2023.113420

Wang, Z., Zhu, H., Gui, J., Zhang, H., Wu, W., Li, Y.: The heat transfer enhancement mechanism for composite phase change material based on variable heating power and pore density. J. Energy Storage. 115, 115954 (2025). https://doi.org/https://doi.org/10.1016/j.est.2025.115954

Nguyen, M.H., Zbair, M., Dutournié, P., Limousy, L., Bennici, S.: Corn Cobs' Biochar as Green Host of Salt Hydrates for Enhancing the Water Sorption Kinetics in Thermochemical Heat Storage Systems. Molecules. 28, (2023). https://doi.org/10.3390/molecules28145381

Lin, J., Zhao, Q., Huang, H.: Performance Analysis of Vermiculite–Potassium Carbonate Composite Materials for Efficient Thermochemical Energy Storage. Energies. 17, (2024). https://doi.org/10.3390/en17122847

Zeng, Y., Clark, R.J., Galazutdinova, Y., Odukomaiya, A., Al-Hallaj, S., Farid, M., Kaur, S., Woods, J.: Open-cycle thermochemical energy storage for building space heating: Practical system

configurations and effective energy density. Appl. Energy. 376, (2024). https://doi.org/10.1016/j.apenergy.2024.124218
Kant, K., Pitchumani, R.: Advances and opportunities in thermochemical heat storage systems for buildings applications, (2022)
Tzinnis, E., Baldini, L.: Combining sorption storage and electric heat pumps to foster integration of solar in buildings. Appl. Energy. 301, (2021). https://doi.org/10.1016/j.apenergy.2021.117455
Pham, A.T., Kinzer, B., Jain, R., Chandran, R.B., Craig, M.T.: Assessing the Value of Coupling Thermal Energy Storage with Air-Source Heat Pumps for Residential Space Heating in U.S. Cities. (2024) https://doi.org/10.48550/arXiv.2407.00527
Aydin, D., Casey, S.P., Riffat, S.: Numerical analysis of solar-assisted seasonal "open" thermochemical heat storage. International Journal of Low-Carbon Technologies. 10, 131–138 (2015). https://doi.org/10.1093/ijlct/ctv005
Miyazaki, T., Akisawa, A., Saha, B.B., El-Sharkawy, I.I., Chakraborty, A.: A new cycle time allocation for enhancing the performance of two-bed adsorption chillers. International Journal of Refrigeration. 32, 846–853 (2009). https://doi.org/10.1016/J.IJREFRIG.2008.12.002
Zhang, W., Yang, Z., Zhang, X., Lv, D., Jiang, N.: Experimental research on the explosion characteristics in the indoor and outdoor units of a split air conditioner using the R290 refrigerant. International Journal of Refrigeration. 67, 408–417 (2016). https://doi.org/10.1016/J.IJREFRIG. 2016.03.018
Aydin, D., Casey, S.P., Chen, X., Riffat, S.: Numerical and experimental analysis of a novel heat pump driven sorption storage heater. Appl. Energy. 211, 954–974 (2018). https://doi.org/10.1016/j.apenergy.2017.11.102
Aristov, Y.I., Restuccia, G., Tokarev, M.M., Buerger, H.-D., Freni, A.: Selective Water Sorbents For Multiple Applications. 11. CaCl 2 Confined To Expanded Vermiculite. Kluwer Academic Publishers (2000) https://doi.org/10.1023/A:1010351815698
Y. A. Çengel and M. A. Boles: Thermodynamics: An Engineering Approach: McGraw-Hill Education. Angewandte Chemie International Edition, 6(11), 951–952. 13, (2015)
Sakoda, A., Suzuki, M.: Simultaneous Transport of Heat and Adsorbate in Closed Type Adsorption Cooling System Utilizing Solar Heat. J. Sol. Energy Eng. 108, 239–245 (1986). https://doi.org/10.1115/1.3268099
Tanashev, Y.Y., Krainov, A. V., Aristov, Y.I.: Thermal conductivity of composite sorbents "salt in porous matrix" for heat storage and transformation. Appl. Therm. Eng. 61, 401–407 (2013). https://doi.org/10.1016/J.Applthermaleng.2013.08.022
Riffat, S., Su, Y., Ding, Y.: Thermochemical cooling system based on adsorption pumping pipe. International Journal of Low-Carbon Technologies. 11, 35–41 (2014). https://doi.org/10.1093/ijlct/ctt055
Wajid, N.M., Mempouo, B., Dodo, A., Omer, S., Riffat, S.B.: Experimental study of an adsorption heat storage systems for building applications. Renewable Bioresources. 4, 2 (2016). https://doi.org/10.7243/2052-6237-4-2
Mempouo, B.: Investigations of Novel Heat Pump Systems for Low Carbon Homes, (2011)
Moffat, R.J.: Describing the Uncertainties in Experimental Results. Exp. Therm. Fluid Sci. (1988) 10.1016/0894-1777(88)90043-X